Inside the Stars, IAU Colloquium 137
ASP Conference Series, Vol. 40, 1993
Werner W. Weiss and Annie Baglin (eds.)

SPIN-DOWN OF SOLAR-TYPE STARS WITH INTERNAL MAGNETIC FIELDS

Paul CHARBONNEAU and Keith B. MACGREGOR High Altitude Observatory, NCAR [1], P.O. Box 3000, Boulder, CO 80307, U.S.A.

ABSTRACT We present a selection of results from a large set of numerical simulations of the spin-down of a solar-type star containing a large scale magnetic field in its radiative interior. Our computations are *dynamical*, in that they take into account both the generation of the toroidal component by the wind-induced shear *and* its back-reaction on the azimuthal flow. Our results demonstrate the existence of classes of internal magnetic fields that can accomodate rapid spin-down near the ZAMS, *and* yield weak internal differential rotation by the solar age.

Keywords: Rotation; Magnetic Fields.

INTRODUCTION

Considerable progress has recently been made toward the goal of identifying and understanding the processes which affect the distribution and evolution of angular momentum in the interiors of the sun and solar-type stars. In particular, the response of the solar interior to the torque applied at its surface by a magnetically coupled wind has been the subject of substantial modeling efforts (see, e.g., Pinsonneault *et al.* 1989; Tassoul & Tassoul 1989; MacGregor & Brenner 1991). However, in considering the internal redistribution of angular momentum, all of these studies have been restricted to purely hydrodynamical (i.e., non-magnetic) transport mechanisms.

The potential importance of large-scale internal magnetic fields in redistributing angular momentum in the stellar radiative interiors has been stressed repeatedly by a number of authors (see, e.g., Mestel & Weiss 1987, and references therein). The mechanism itself is simple: a shear in the azimuthal flow, acting on a pre-existing large-scale poloidal magnetic field, will generate a toroidal magnetic component, with which is associated a Lorentz force in the ϕ-direction, itself acting in such a way as to oppose the driving shear. However, a consistent quantitative study of this process is still lacking. A number of questions that come to mind are: (Q1) How do internal magnetic fields affect the surface rotational evolution ? (Q2) What level of internal differential rotation can they tolerate ? (Q3) What is the strength of the toroidal field generated ? (Q4) What is the time-evolution of the internal toroidal field ? (Q5) To what degree are answers to Q1—Q4 affected by the assumed strength and geometry of the internal poloidal field ? Our purpose is to provide *quantitative* answers to the above questions, in the context of the solar spin-down problem.

[1] The National Center for Atmospheric Research is sponsored by the National Science Foundation.

MODEL ASSUMPTIONS AND SELECTED RESULTS

Our formulation of the spin-down problem is based on the following working assumptions: (A1) Axisymmetric system (rotation and magnetic axes parallel), (A2) Time-independent poloidal magnetic field, (A3) No fluid motion in meridional planes, (A4) Constant kinematic viscosity and magnetic diffusivity, (A5) No Coriolis forces, (A6) Static stellar envelope model, (A7) Solid-body rotation in convective envelope (hereafter "CE"), and (A8) Solid-body rotation and zero toroidal field on the ZAMS.

In view of A1, A2 and A3, we have $\mathbf{U} = \Omega(r,\theta,t)\, r\, sin\theta\, \hat{\mathbf{e}}_\phi$, and $\mathbf{B} = \mathbf{B}_p(r,\theta) + B_\phi(r,\theta,t)\,\hat{\mathbf{e}}_\phi$. The spin-down problem reduces to solving the (linear but coupled) ϕ-components of the momentum and induction equations. The angular momentum loss rate is computed using the Weber & Davis (1967) axisymmetric formulation (see also Belcher & MacGregor 1976). We model angular momentum loss as a sink within the CE, rather than a torque at the surface. Solutions to the governing equations are obtained using the finite element-based numerical scheme describe in Charbonneau & MacGregor (1992*a*, appendix). We use a standard solar model computed by R. Gilliland. The model reaches the ZAMS at $t_{ZAMS} \simeq 4 \times 10^7$ yrs, at which time the core-envelope boundary is located at $R_{CE} = 0.74 R_\odot$, and the CE accounts for about 10% of the total moment of inertia.

The internal rotational and magnetic evolution can be subdivided in three more or less distinct epochs. The first is of short duration, corresponding to the buildup of the toroidal fields in the radiative interior following the shearing of the pre-existing poloidal field. The second epoch, especially for magnetic configurations having direct magnetic coupling at the core-envelope interface, is characterized by the presence of vigorous *phase mixing* (see e.g. Roxburgh, 1991). This results in the damping of the torsional Alfvén waves generated earlier. The third epoch of evolution is characterized by a state of approximate dynamical balance such that the total stresses (magnetic + viscous) at the core-envelope interface equilibrate almost exactly the wind-induced surface torque. The system essentially evolves on the Alfvén timescale (of order 10^3—10^4 yrs for a $||\mathbf{B}_p|| \simeq 1$ G) during epochs 1 and 2, but on the wind braking timescale during epoch 3. This leads to a quasi-static internal and magnetic evolution from about 10^7 yrs all the way to the solar age.

Figure 1 [Plate] shows a few snapshots of the internal evolution for three different internal poloidal fields (all of average strength 1 G). The color scale codes B_ϕ, and the contour lines the azimuthal velocity u_ϕ ($= \Omega\, r\, sin\theta$; see caption for details). The portion of the envelope threaded by fieldlines that close upon themselves within the radiative zone is magnetically decoupled from the rest of the envelope, and tends to rotationally lag behind the CE, thus acting as a reservoir of angular momentum. Note the high strength of the toroidal magnetic fields generated during the early epochs of spin-down. For all configurations, toroidal field strengths reach a maximum around the Pleiades age ($t + t_{ZAMS} \simeq 70$ Myr), and decrease monotonically thereafter.

Figure 2 shows the evolution in time of the surface rotation rate for solutions of various internal field geometries and strengths. The extremely weak dependence of surface rotational evolution on field strength, for some configurations (D2 and D4), is noteworthy. In the case of D2, it is a direct consequence of the aforementioned dynamical balance at the core-envelope

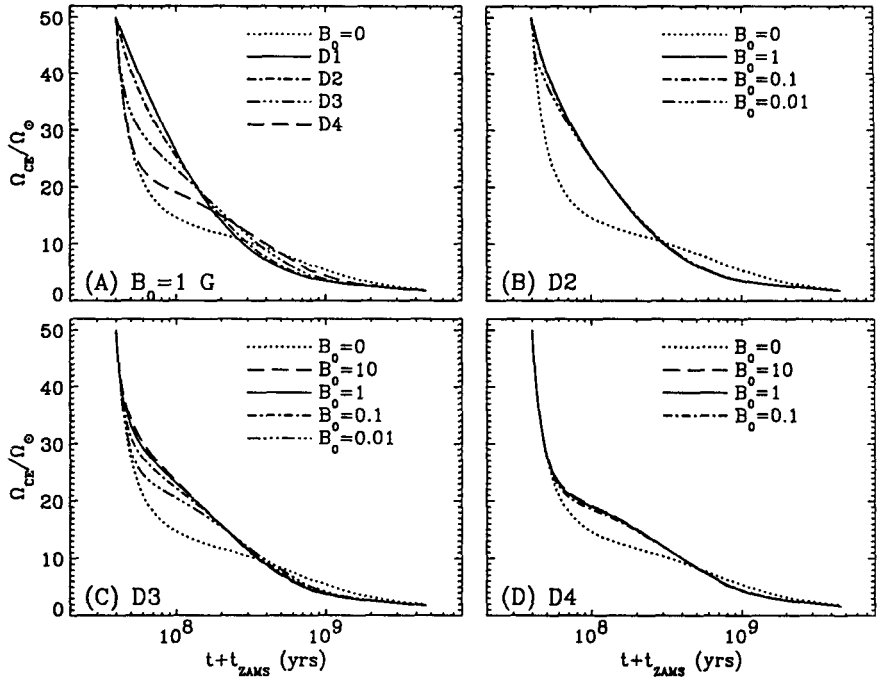

Figure 2 : Selected surface rotational evolution curves for a solar model. Part (A) shows results for a fixed poloidal fields strengths and various degrees of core-envelope magnetic coupling (see Fig. 1 [Plate]), and parts (B) (C) and (D) shows results for a fixed degree of coupling but various field strengths. Note the convergence of surface rotations rate beyond $t \sim 10^9$ yrs.

interface. The greater dependence on field strength, for the D3 configuration in the first few 10^8 yrs of evolution, reflects the influence of the poloidal field on the viscous boundary layer forming at the core-envelope interface for this field geometry. Similar results are obtained for quadrupolar internal fields.

Figure 3 shows the time evolution of internal differential rotation. The dimensionless quantity $\Delta\Omega$, is a *global* measure, obtained by integrating $\Omega(r,\theta,t) - \Omega_{CE}(t)$ over the magnetized part of the radiative core. Note on Fig. 3 how $\Delta\Omega$ reaches a maximum around $t + t_{ZAMS} \simeq 10^8$ yrs, and gradually decreases thereafter, down to $\Delta\Omega \sim 10\%$ by the solar age.

CONCLUSIONS

A detailed examination of our solutions yields the following conclusions (Charbonneau & MacGregor, 1992b; Charbonneau & MacGregor, in preparation; MacGregor, these proceedings): (C1) The presence of magnetic fields in radiative interiors is compatible with the observed rapid-down of solar analogs observed in young clusters (for a subset of poloidal field geometry). (C2) The surface rotational evolution is weakly dependent on the assumed internal poloidal field strength. (C3) The presence of magnetic fields leads to low internal angular

https://doi.org/10.1017/S0252921100018261 Published online by Cambridge University Press

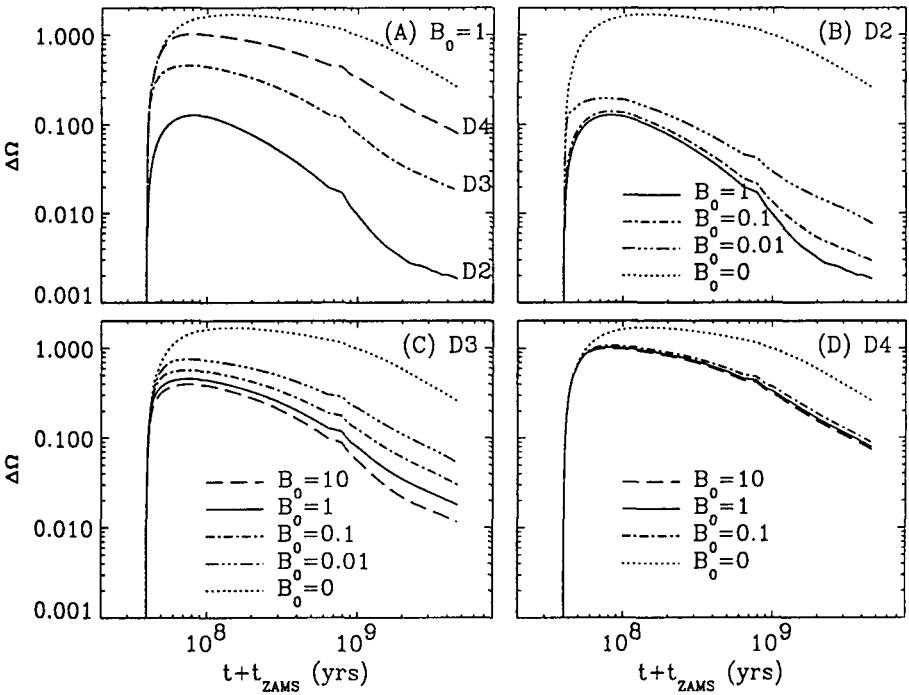

Figure 3 : Time-evolution of the internal differential rotation, for the same solutions as shown on Fig. 2. Note how even for configurations without direct magnetic coupling at the core-envelope interface (D3 and D4), $\Delta\Omega$ has fallen below 10% for most field strengths.

velocity gradients in radiative interiors by the solar age. (C4) The spin-down of solar-type stars generates strong (i.e, tens, sometimes hundreds of kG) toroidal magnetic fields in their radiative interiors. (C5) Toroidal oscillations set up at early epochs have large amplitudes in B_ϕ, very low amplitude in Ω, and are rapidly (within a few 10^5 yrs) damped via phase mixing. (C6) The present photospheric solar rotation is a very poor indicator of the strength and geometry (past and present) of the solar internal magnetic field. (C7) The present internal solar differential rotation is a much better probe of the solar internal magnetic field.

REFERENCES

Belcher, J.W., & MacGregor, K.B. 1976, *Ap. J.*, **203**, 720
Charbonneau P., & MacGregor K.B. 1992a, *Ap. J.*, **387**, 639 (paper I)
Charbonneau P., & MacGregor K.B. 1992b, submitted to ApJ.
MacGregor, K. B., & Brenner, M. 1991, *Ap. J.*, **376**, 204
Mestel, L., & Weiss, N.O. 1987, *M. N. R. A. S.*, **226**, 123
Pinsonneault, M.H., Kawaler, S.D., Sofia, S., & Demarque, P. 1989, *Ap. J.*, **338**, 424
Roxburgh, I.W. 1991, in *Angular Momentum Evolution of Young Stars*, eds. S. Catalano & J. Stauffer (Dordrecht: Kluwer Academic Publishers), p. 365.
Tassoul, J.-L., & Tassoul, M. 1989, *Astr. Ap.*, **213**, 397
Weber, E.J., & Davis, L. Jr. 1967, *Ap. J.*, **148**, 217

https://doi.org/10.1017/S0252921100018261 Published online by Cambridge University Press

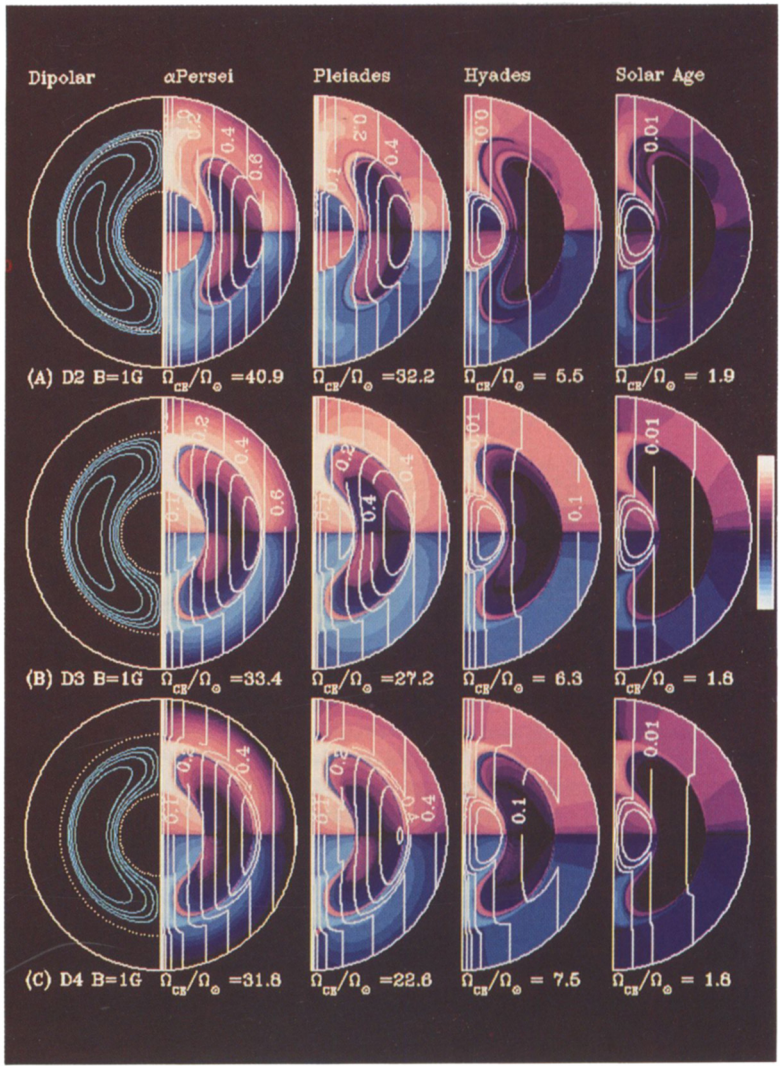

Figure 1 : Internal toroidal magnetic field and rotational profile at a few selected epochs. The blue—cyan sequence codes $log(+B_\phi)$, and the blue—pink sequence $log(-B_\phi)$ (with a lower cutoff at $|B_\phi| \leq 1$ G). The contour lines code the dimensionless azimuthal velocity u_ϕ $[= (\Omega/\Omega_0)(r\ sin\,\theta/R_*) =$ 0.005, 0.01, 0.02, 0.05, 0.1, 0.2, 0.3, 0.4, 0.5, 0.6, 0.7, 0.8, 0.9 and 1.0]. Solutions are shown for three different poloidal field configurations, the corresponding fieldlines being shown at the extreme left in each row. Note that direct magnetic coupling (i.e., $B_r \neq 0$ for some θ at $r = R_{CE}$) exists only for the D2 configuration (first row). We have adopted $t + t_{ZAMS} =$ 0.05, 0.07, 0.6 and 4.6 Gyrs for the ages of αPersei, the Pleiades, Hyades, and the Sun.

https://doi.org/10.1017/S0252921100018261 Published online by Cambridge University Press